Electronic Supplementary Material (ESI) for Catalysis Science & Technology.
This journal is © The Royal Society of Chemistry 2020

Effect of catalyst morphology and hydrogen co-feeding on the acid-catalysed transformation of acetone into mesitylene

*Jorge Quesada, Laura Faba, Eva Díaz, and Salvador Ordóñez**

Catalysis, Reactors and Control Research Group (CRC), Dept. of Chemical and Environmental Engineering, University of Oviedo, Oviedo 33006, Spain

SUPPLEMENTARY INFORMATION

Contents **Page**

Assessment of external and internal diffusional resistances to acetone transfer

Based on experimental data in inert conditions, the external diffusion was evaluated using the Mear's coefficient (C_M) (**Eq. S1**; Mear's criterion: if $C_M < 0.15$, external mass transfer effects can be neglected) while the internal diffusion was assessed by both the Thiele modulus (ϕ) and the effectiveness factor (η) through the Weisz-Prater parameter (C_{WP}) (**Eqs. S2-S3**).[1] Results, summarized in **Table S1**, indicate that the external convective resistance is negligible. In fact, for all tested materials, the Mear's criterion is fulfilled, obtaining values up to four order of magnitude lower than threshold (0.15). On the other hand, internal resistance diffusion cannot be ruled out in any case. The lowest mass transfer effects of internal diffusion hindrance are observed for the MCM-41, with an effectiveness factor close to 80%. However, internal diffusion limits the reaction rate practically at all in the case of zeolites, especially for the MFI structure (η < 1%). This behavior is due to the similarity in size between the acetone molecule and the material channels that governs the Knudsen diffusion (which decreases as well as this size difference decreases). **Table S2** include operational conditions, physical properties of the gas-phase, and materials' properties.

$$C_M = (r\rho_b d_c n)/(2k_c[A]) < 0.15 \quad \text{(S1)}$$

$$C_{WP} = \eta\phi^2 = (r\rho_c {d_c}^2)/(4D_{eA}[A]_s) \quad \text{(S2)}$$

$$\eta\cdot\phi^2 = 3(\phi\coth(\phi) - 1) \quad \text{(S3)}$$

where r = acetone reaction rate (mol kg^{-1} s^{-1}). In this case, it is the acetone reaction rate at zero time of reaction (r_0).

ρ_b = bulk density (kg m^{-3}).

d_c = diameter of the catalyst particles (m), considering spherical geometry.

$[A]$ = acetone concentration in the gas-phase (mol m^{-3}); otherwise, sub-index s means acetone concentration on the catalyst surface. If external diffusional effects are negligible, then $[A]_s$ = $[A]$. The considered $[A]$ are those for the worst-case scenario (*i.e.*, reaction outgoing gas-phase) for each sample at zero time of reaction. Therefore, it is determined by the following equation: $[A] = [A]_i(1 - x_0)$, being $[A]_i$ the acetone concentration of the inlet stream and x_0 the acetone conversion at zero time of reaction (included in **Table 2**).

n = reaction order. A value of 2 is considered for the acetone reaction rate equation, since the acetone bimolecular aldolization reaction is the first one of the proposed reaction pathways (**Scheme 1**) and the aldolization is also deemed as the kinetically-relevant elementary step in aldol condensation reactions.[2]

k_c = mass transfer coefficient (m s^{-1}). It is determined by the dimensionless Sherwood number (Sh) (**Eq. S4**), which, in turn, is estimated through the Frössling correlation for mass transfer around spherical particles (**Eq. S5**). For this purpose, the dimensionless Reynolds (Re) and Schmidt (Sc) numbers need to be calculated (**Eqs. S6-S7**).[3]

ρ_c = catalyst density (kg m^{-3}).

D_{eA} = effective diffusivity of acetone in the gas mixture (m^2 s^{-1}). It is quantified by a correction of the diffusion coefficient of acetone in the gas mixture (D_A) through the catalyst porosity (ε_c) and tortuosity (τ) (**Eq. S8**). Values of τ are estimated through the ε_c using the **Eq. S9**.[4] For the determination of D_A, it is considered helium and acetone, but not reaction products (this assumption is underpinned by the differential reaction conditions, *i.e.*, low acetone conversion). In this context, the gas-phase consists of a binary mixture with equimolar counter-diffusion and, therefore, D_A can be estimated by the Bosanquet equation (**Eq. S10**).[5] The binary diffusion coefficient (D_{AB}) is calculated by the method of Fuller *et al.*,[6] while the Knudsen diffusivity (D_K) is determined by the **Eq. S11**.[5]

$$Sh = k_c d_c / D_{AB} \tag{S4}$$

$$Sh = 2 + 0.6 Re^{1/2} Sc^{1/3} \tag{S5}$$

$$Re = u \rho_G d_c / \mu \tag{S6}$$

$$Sc = \mu / \rho_G D_{AB} \tag{S7}$$

$$D_{eA} = \varepsilon_c D_A / \tau \tag{S8}$$

$$\tau = (1 + \varepsilon_c)^2 / [\varepsilon_c (1 + \varepsilon_c)^2 + 4 {\varepsilon_c}^2 (1 - \varepsilon_c)] \tag{S9}$$

$$D_A = ({}^{1}/{D_{AB}} + {}^{1}/{D_K})^{-1} \tag{S10}$$

$$D_K = (d_p/3) \sqrt{{}^{8RT}/{\pi M_A}} \tag{S11}$$

where u = free-stream velocity (m s^{-1}).

ρ_G = gas-phase density (kg m^{-3}). It is determined through the ideal gas law for the reaction conditions tested.

μ = gas-phase viscosity (Pa s). It is estimated using the method of Wilke for a binary system of helium and acetone from their respective viscosities at operational conditions.[7]

d_p = material pore size (m). It is considered the pore-limiting diameter (d_{PL}) for each material (summarized in **Table 1**).

R = ideal gas constant (J mol^{-1} K^{-1}).

T = temperature of operation (K).

M_A = acetone molar mass (kg mol^{-1}).

The hydraulic regime has been corroborated, according to the modified Reynolds number for catalytic beds, taking into account the free space due to the bed porosity.

$$Re' = u\rho_G d_c/(\mu\cdot(1-\varepsilon)) \tag{S7}$$

Considering this expression, values lower than 10 indicate a laminar flow, whereas values higher than 100 guarantee a turbulent flow. Results are summarized in Table S1, obtained in all the cases values higher than 480. According to this, the laminar flow is discarded, assuming the conditions of a plug-flow reactor. In the same way, according to the classical criteria provided by Satterfield[8], axial dispersion is negligible if the ratio between reactor length and reactor diameter is higher than 50, being a minimum of a 20% higher in our case.

References

1. H. S. Fogler, In *Elements of Chemical Reaction Engineering*, 4th ed., Prentice Hall, Westford, 2006; p. 839-841.
2. S. Wang, K. Goulas and E. Iglesia, *J. Catal.*, 2016, **340**, 302-320.
3. H. S. Fogler, In *Elements of Chemical Reaction Engineering*, 4th ed., Prentice Hall, Westford, 2006; p. 774-776.
4. W. Kong, Q. Zhang, X. Xu and D. A. Chen, *Energies*, 2015, **8**, 13953-13959.
5. G. F. Froment, K. B. Bischoff and J. De Wilde, In *Chemical Reactor Analysis and Design*, 3rd ed., John Wiley & Sons, Inc., Hoboken, 2011; p. 174-177.
6. B. E. Poling, J. M. Prausnitz and J. P. O'Connell, In *The Properties of Gases and Liquids*, 5th ed., McGraw-Hill, New York, 2001; Chapter 11, p. 10.
7. B. E. Poling, J. M. Prausnitz and J. P. O'Connell, In *The Properties of Gases and Liquids*, 5th ed., McGraw-Hill, New York, 2001; Chapter 9, p. 21.

8. C.N. Satterfield, *Heterogeneous Catalysis in Industrial Practice*, 2nd ed., Krieger Pub.Co., Malabar FL, 1996; Chapter 11, p. 497.

Table S1. Results obtained from the evaluation of external and internal diffusional resistances to acetone transfer based on experimental data for the gas-phase acetone self-condensation at 573 K in inert conditions (WHSV = 7.8 h-1).

Material	r_0 (mol kg^{-1} s^{-1}), 10^3	C_M, 10^5	C_{WP}	ϕ	η (%)	Re
MCM-41	4.2	8.1	3.4	2.1	79.5	481
MFI1	1.6	2.8	979.4	327.5	0.9	507
MFI2	3.5	5.0	2588.7	863.9	0.3	568
BEA	6.8	13.3	63.0	22.0	13.0	541

Table S2. Operational conditions, physical properties of the gas-phase, and catalysts' properties used in the gas-phase acetone self-condensation in inert conditions.

Parameter		
P (kPa)		101.3
T (K)		573
$[A]_i$ (mol m^{-3})		4.3
WHSV (h^{-1})		7.8
u (m s^{-1}), 10		1.3
ρ_G (kg m^{-3}), 10		3.2
μ (Pa s), 10^5		2.3
M_A (kg mol^{-1}), 10^2		5.8
Property	**Material**	
ρ_b (kg m^{-3}), 10^{-2}	MCM-41	2.3
	MFI1	2.2
	MFI2	1.7
	BEA	2.1

ρ_c (kg m^{-3}), 10^{-2}	MCM-41	6.1
	MFI1	3.2
	MFI2	2.7
	BEA	4.2
ε_c	MCM-41	0.50
	MFI1	0.03
	MFI2	0.03
	BEA	0.25

Table S3. Disaggregated selectivities of the compounds lumped under the C6 and C9 pools in the gas-phase acetone self-condensation at 573 K in inert conditions (WHSV = 7.8 h^{-1}) using MCM-41 aluminosilicate as catalyst. (MO: mesityl oxide; IMO: isomesityl oxide; P: phorones; IP: isophorones; M: mesitylene).

TOS (h)	C6-pool		C9-pool		
	φ_{MO} (%)	φ_{IMO} (%)	φ_P (%)	φ_{IP} (%)	φ_M (%)
0.61	6.3	1.6	0	3.2	14.8
1.21	8.2	2.1	0.8	3.7	16.4
1.81	10.5	2.6	0.9	3.5	17.8
2.42	11.3	2.8	1.1	3.9	18.4
3.06	12.1	3.1	1.2	3.8	18.5
3.67	12.8	3.3	1.9	3.8	18.5
4.28	13.9	3.5	1.4	4.3	19.3
4.91	14.8	3.7	1.5	4.5	19.5
5.55	15.2	3.9	1.4	4.4	19.9
6.19	16.0	4.0	1.3	4.6	20.4

Table S4. Disaggregated selectivities of the compounds lumped under the C6 and C9 pools in the gas-phase acetone self-condensation at 573 K in inert conditions (WHSV = 7.8 h^{-1}) using MFI1 zeolite as catalyst. (MO: mesityl oxide; IMO: isomesityl oxide; P: phorones; IP: isophorones; M: mesitylene).

TOS (h)	C6-pool		C9-pool		
	φ_{MO} (%)	φ_{IMO} (%)	φ_{P} (%)	φ_{IP} (%)	φ_{M} (%)
0.53	8.8	2.3	0	0.8	1.8
1.17	13.9	3.6	0	0.8	3.0
1.79	16.4	4.2	0	0.9	3.4
2.43	18.3	4.7	0	1.0	3.7
3.06	20.7	5.3	0	1.1	4.0
3.71	21.9	5.6	0	1.1	4.2
4.36	22.3	5.7	0	1.2	4.1
5.02	24.5	6.2	0	1.2	4.4
5.69	24.4	6.2	0	1.2	4.4

Table S5. Disaggregated selectivities of the compounds lumped under the C6 and C9 pools in the gas-phase acetone self-condensation at 573 K in inert conditions (WHSV = 7.8 h^{-1}) using MFI2 zeolite as catalyst. (MO: mesityl oxide; IMO: isomesityl oxide; P: phorones; IP: isophorones; M: mesitylene).

TOS (h)	C6-pool		C9-pool		
	φ_{MO} (%)	φ_{IMO} (%)	φ_{P} (%)	φ_{IP} (%)	φ_{M} (%)
0.54	1.6	0.4	0	0.2	0
1.26	3.1	0.8	0	0.3	0
1.94	4.2	1.1	0	0.3	0
2.62	5.1	1.3	0	0.4	0
3.30	4.4	1.1	0	0.5	0
3.98	5.9	1.5	0	0.4	0
4.63	6.8	1.8	0	0.5	0
5.30	7.6	2.0	0	0.5	0
5.93	7.8	2.0	0	0.5	0

Table S6. Disaggregated selectivities of the compounds lumped under the C6 and C9 pools in the gas-phase acetone self-condensation at 573 K in inert conditions (WHSV = 7.8 h^{-1}) using BEA zeolite as catalyst. (MO: mesityl oxide; IMO: isomesityl oxide; P: phorones; IP: isophorones; M: mesitylene).

TOS (h)	C6-pool		C9-pool		
	φ_{MO} (%)	φ_{IMO} (%)	φ_{P} (%)	φ_{IP} (%)	φ_{M} (%)
0.52	3.6	0.9	0.5	2.3	9.3
1.13	8.4	2.2	0.1	2.0	11.5
1.74	12.0	3.1	0.2	2.1	12.8
2.34	13.4	3.4	0.2	2.0	13.1
2.94	14.4	3.7	0.2	2.1	13.3
3.54	15.8	4.1	0.3	2.4	13.9
4.13	15.6	4.1	0.2	2.0	13.4
4.75	18.4	4.7	0.2	2.2	14.3
5.34	17.1	4.4	0.2	2.1	13.6
5.93	18.2	4.7	0.3	2.1	14.0

Table S7. Disaggregated selectivities of the compounds lumped under the C6 and C9 pools in the gas-phase acetone self-condensation at 573 K in presence of H_2 (WHSV = 7.8 h^{-1}) using MCM-41 aluminosilicate as catalyst. (MO: mesityl oxide; IMO: isomesityl oxide; MIBK: methyl isobutyl ketone; P: phorones; IP: isophorones; M: mesitylene; DIBK: diisobutyl ketone).

TOS (h)	C6-pool			C9-pool			
	φ_{MO} (%)	φ_{IMO} (%)	φ_{MIBK} (%)	φ_{P} (%)	φ_{IP} (%)	φ_{M} (%)	φ_{DIBK} (%)
0.50	5.4	1.2	0.6	6.9	14.7	23.6	1.6
1.14	7.8	1.7	0.6	8.8	14.3	24.3	1.1
1.81	9.4	2.0	0.5	7.8	15.9	25.5	1.0
2.44	11.1	2.4	0.5	8.2	13.4	26.4	0.8
3.07	11.4	2.4	0.5	7.8	16.2	27.9	0.8
3.68	12.0	2.6	0.5	7.1	15.9	27.9	0.8
4.30	13.8	2.9	0.4	6.9	15.6	29.2	0.7

Table S8. Disaggregated selectivities of the compounds lumped under the C6 and C9 pools in the gas-phase acetone self-condensation at 573 K in presence of H_2 (WHSV = 7.8 h^{-1}) using BEA zeolite as catalyst. (MO: mesityl oxide; IMO: isomesityl oxide; MIBK: methyl isobutyl ketone; P: phorones; IP: isophorones; M: mesitylene; DIBK: diisobutyl ketone).

TOS (h)	C6-pool			C9-pool			
	φ_{MO} (%)	φ_{IMO} (%)	φ_{MIBK} (%)	φ_{P} (%)	φ_{IP} (%)	φ_{M} (%)	φ_{DIBK} (%)
0.57	3.6	0.7	0.4	10.4	11.8	18.6	3.8
1.19	9.7	2.0	0.3	6.7	10.8	22.4	2.2
1.82	11.5	2.4	0.2	6.4	11.5	23.7	1.9
2.46	12.8	2.7	0.2	6.0	12.6	23.3	1.7
3.11	14.6	3.0	0.2	5.4	12.4	24.6	1.5
3.75	14.8	3.1	0.2	6.1	13.1	24.5	1.5
4.39	15.9	3.3	0.2	5.5	12.5	24.4	1.4

Table S9. Evolution of the relative selectivity to isophorones and mesitylene with regard to their respective C9 precursors in the gas-phase acetone self-condensation at 573 K in both absence and presence of H_2 (WHSV = 7.8 h^{-1}) with MCM-41 and BEA aluminosilicates. (P: phorones; IP: isophorones; M: mesitylene).

MCM-41[a]			MCM-41[b]			BEA[a]			BEA[b]		
TOS (h)	φ_{IP}/φ_P	$\varphi_M/(\varphi_P+\varphi_{IP})$	TOS (h)	φ_{IP}/φ_P	$\varphi_M/(\varphi_P+\varphi_{IP})$	TOS (h)	φ_{IP}/φ_P	$\varphi_M/(\varphi_P+\varphi_{IP})$	TOS (h)	φ_{IP}/φ_P	$\varphi_M/(\varphi_P+\varphi_{IP})$
0.61	-	4.7	0.50	2.1	1.1	0.52	4.8	3.3	0.57	1.1	0.8
1.21	4.6	3.6	1.14	1.6	1.1	1.13	13.5	5.5	1.19	1.6	1.3
1.81	4.1	4.1	1.81	2.1	1.1	1.74	11.0	5.7	1.82	1.8	1.3
2.42	3.5	3.6	2.44	1.6	1.2	2.34	12.9	6.0	2.46	2.1	1.3
3.06	3.2	3.7	3.07	2.1	1.2	2.94	11.4	5.9	3.11	2.3	1.4
3.67	2.1	3.3	3.68	2.3	1.2	3.54	7.1	5.1	3.75	2.1	1.3
4.28	3.1	3.4	4.30	2.3	1.3	4.13	-	6.8	4.39	2.3	1.4

[a] Inert conditions.

[b] H_2 co-feeding conditions.

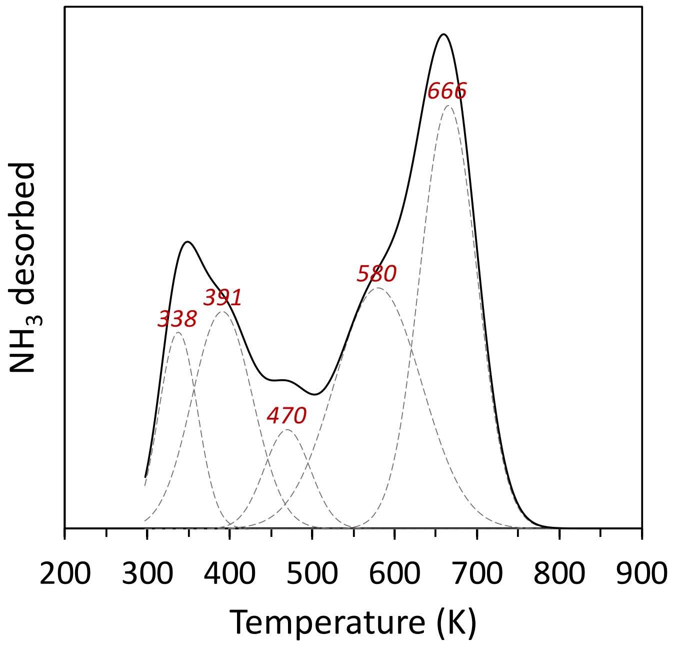

Figure S1. TPD-MS profile of the NH_4^+-MFI1 zeolite during the flowing-air thermal treatment to H^+-MFI1 sample.

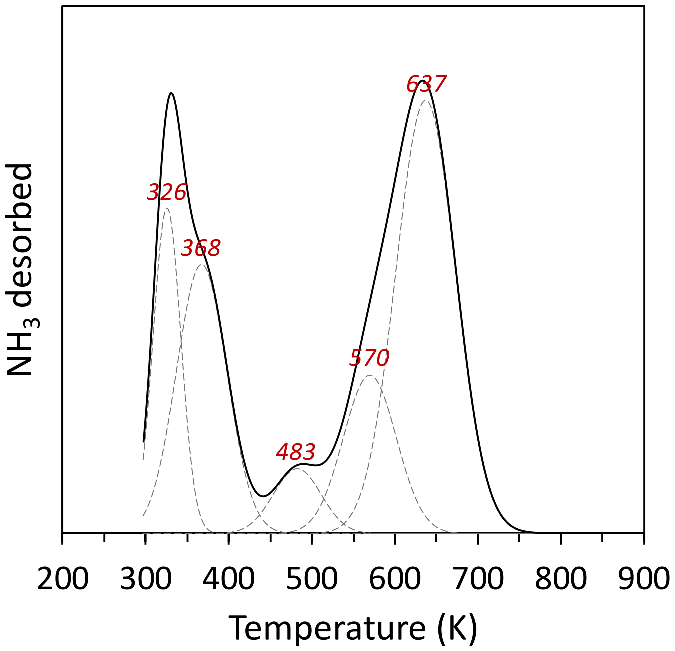

Figure S2. TPD-MS profile of the NH_4^+-MFI2 zeolite during the flowing-air thermal treatment to H^+-MFI2 sample.

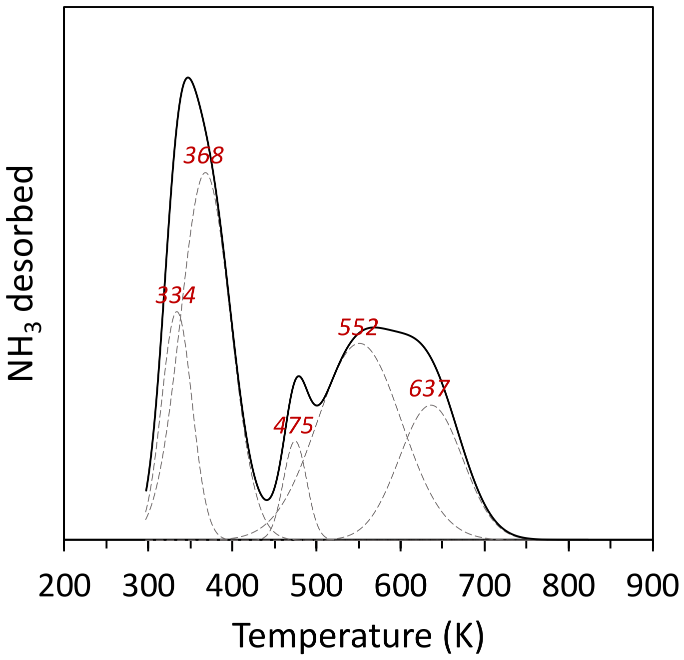

Figure S3. TPD-MS profile of the NH_4^+-BEA zeolite during the flowing-air thermal treatment to H^+-BEA sample.

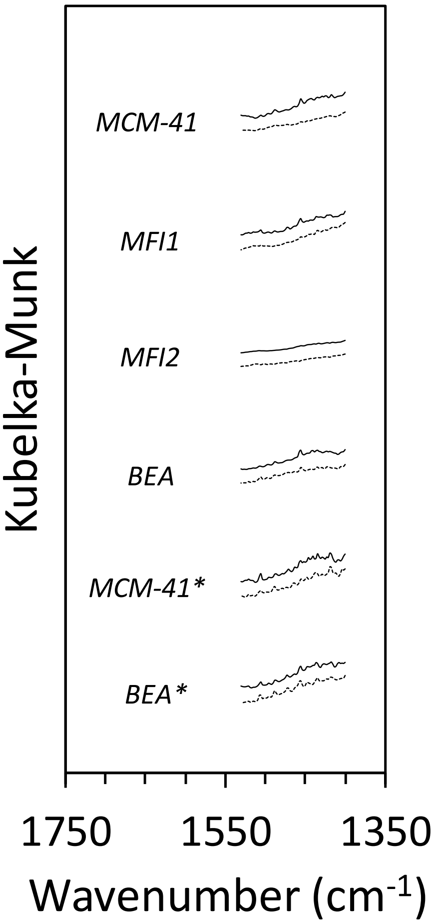

Figure S4. DRIFT spectra obtained in the gas-phase acetone self-condensation for the band linked to νC-C and δCHH of mesitylene. Dashed lines: 0.5 h; solid lines: 4 h. * Results corresponding to H_2 co-feeding experiments.